IMPLANTABLE PARYLENE-BASED WIRELESS INTRAOCULAR PRESSURE SENSOR

Po-Jui Chen[1], *Damien C. Rodger*[2], *Saloomeh Saati*[3], *Mark S. Humayun*[2,3], *and Yu-Chong Tai*[1]
[1]California Institute of Technology, Pasadena, CA, USA
[2]University of Southern California, Los Angeles, CA, USA
[3]Doheny Eye Institute, Los Angeles, CA, USA

ABSTRACT

This paper presents a novel implantable, wireless, passive pressure sensor for ophthalmic applications. Two sensor designs incorporating surface-micromachined variable capacitor and variable capacitor/inductor are implemented to realize the pressure sensitive components. The sensor is monolithically microfabricated using parylene as a biocompatible structural material in a suitable form factor for increased ease of intraocular implantation. Pressure responses of the microsensor are characterized on-chip to demonstrate its high pressure sensitivity (> 7000 ppm/mmHg) with mmHg level resolution. An *in vivo* animal study verifies the biostability of the sensor implant in the intraocular environment after more than 150 days. This sensor will ultimately be implanted at the pars plana or iris of the eye to fulfill continuous intraocular pressure (IOP) monitoring in glaucoma patients.

1. INTRODUCTION

Intraocular pressure (IOP) monitoring is crucial in the management of glaucoma patients as it is known one of the most effective methods to evaluate the progression of this chronic eye disease [1]. Applanation tonometry using contact or non-contact approach is the current clinical technique for IOP recording. However, it has difficulties in providing reliable and repeatable measurements and, particularly, in deployment for continuous tracking, which impedes prompt detection and appropriate treatment for IOP spikes considered as a separate risk factor to optic nerve damage. Continuous IOP monitoring in glaucoma patients with high accuracy and high reliability is therefore a consistent need for ophthalmologists.

Passive telemetric sensing is one of the viable methods for continuous and faithful non-contact IOP measurements. The concept as shown in Fig. 1 was first proved in 1967 using a sensor with resonant circuitry implanted to the anterior chamber of the eye [2]. By wirelessly interrogating the sensor through an inductive coupling link, an external reader can register IOP variations without indirect derivation and calculations as are used in applanation tonometry. Enabled by microfabrication technologies, a miniaturized wireless sensor was later reported with its application for IOP monitoring as well [3]. The model has been more completely studied given the development of various pressure microsensors [4-7], with a needle-implantable flexible sensor for pressure monitoring of abdominal aortic aneurysms (AAA) as a specific example for biomedical applications. On the technology side, however, all these paradigms involve delicate multiple wafer fabrication with wafer bonding as the essential process. In this work, with the knowledge of utilizing parylene in surface-micromachined capacitive sensors [8], we investigate a monolithically microfabricated parylene-based sensor in a form factor favorable for minimally invasive ocular implantation. Featuring parylene as the biocompatible polymeric material, the pressure sensor is designed to be completely implantable in the intraocular environment so that long-term IOP monitoring of glaucoma patients can be fulfilled.

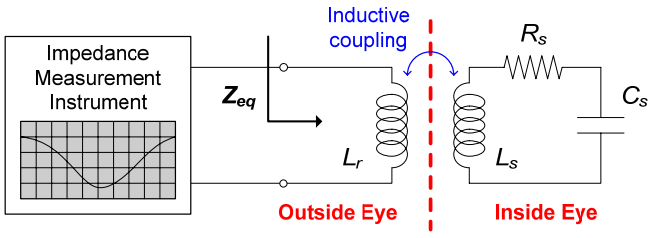

Figure 1. *Conceptual schematic of passive wireless IOP sensing. The implanted sensor can register faithful pressure variations using corresponding electrical characteristic changes, which are measured from the external reader through a wireless inductive coupling link.*

2. DESIGN

Device Structure

The proposed pressure sensor as shown in Fig. 2 comprises a flexible diaphragm chamber integrated with parallel metal plates as an integrated capacitor and metal wires as a dual-layer planar inductor to create the resonant circuit that communicates with the external reader. A deformable diaphragm with embedded electrical components enables gauge pressure sensing of the device. For instance, a pressure sensitive variable capacitor can be realized by arranging the bottom plate on the substrate and the top plate in the diaphragm. In addition to a fixed inductor surrounding the variable capacitor, a variable inductor can also be realized by embedding the top metal wire layer in the diaphragm to alter the mutual inductance between two planar inductors for further enhanced overall pressure sensitivity. These two designs are implemented on a monolithic substrate with the use of surface-micromachining technology so as to have less fabrication complexity compared with wafer bonding technology. All device structures including oxidized silicon substrate, titanium/gold metal lines and plates, and parylene diaphragm are made out of biocompatible materials to ensure the feasibility of device implantation. Parylene C (poly-para-xylylene C) is selected as the diaphragm material because of its mechanical flexibility (Young's modulus ~4

GPa), CMOS/MEMS processes compatibility, and biocompatibility (FDA approved USP Class VI grade). Its room-temperature conformal deposition nature allows large diaphragm chambers to be easily and reliably formed on a monolithic substrate. Additionally, its dielectric property (dielectric constant ~2.95 at 1 MHz) makes parylene C a straightforward insulator between metal layers.

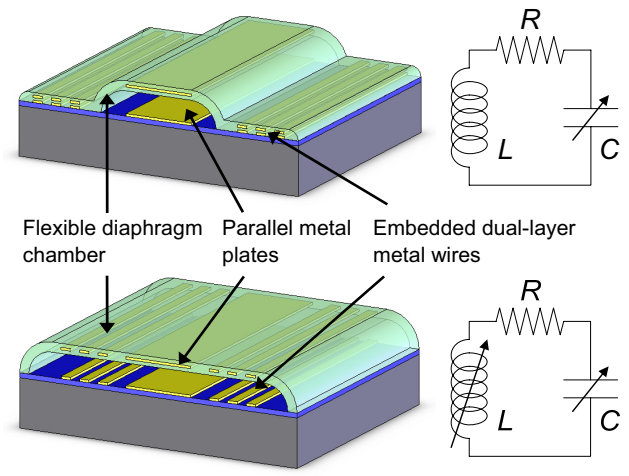

Figure 2. *Sensor design: (top) Variable capacitor; (bottom) Variable capacitor/inductor. The deformable diaphragm chamber with respect to pressure changes realizes pressure sensitive electrical characteristics of the sensors.*

Circuit Analysis

In the lumped model illustrated in Fig. 1, the equivalent impedance as viewed from the measurement instrument can be written as [4-7]:

$$Z_{eq} = \frac{V}{I} = j2\pi fL_r \left[1 + k^2 \frac{\left(\frac{f}{f_o}\right)^2}{1 - \left(\frac{f}{f_o}\right)^2 + \frac{1}{Q_s} j \frac{f}{f_s}} \right]$$

$$= j2\pi fL_r \left(1 + jk^2 Q_s\right) \quad \text{when} \quad f = f_s$$

where $f_s = [2\pi(L_sC_s)^{1/2}]^{-1}$ is the sensor resonant frequency and $Q_s = R_s^{-1}(L_sC_s^{-1})^{1/2}$ is the quality factor of the sensor at resonance, and k is the coupling coefficient of the inductive link. This equation implies that a phase-dip technique can be applied to detect the resonant frequency of the sensor as the phase of the equivalent impedance drops to the minimum with an approximate dip magnitude:

$$\Delta\phi \cong \tan^{-1}\left(k^2 Q_s\right) \quad \text{when} \quad f = f_s \ .$$

As a result, the changes of resonant frequency with respect to pressure variations experienced by the sensor can be registered *in situ* by observing the shift of phase dip in frequency domain so that continuous environmental pressure monitoring can be accomplished. Electrical characteristics including inductance, resistance, and capacitance of the sensor were calculated using theoretical equations [9][10], so that the overall sensing performance can be estimated meeting the specification in miniature pressure variation measurement (± 1 mmHg) for accurate IOP monitoring.

3. FABRICATION

The fabrication process illustrated in Fig. 3 started by thermally growing and patterning 0.75 µm oxide on a double-side-polished silicon wafer as an insulation layer. In frontside processes, e-beam-evaporated metals were used here for better material quality purposes while thick deposition was required to obtain low overall resistance from the metal wires. A thick titanium/gold (200 Å/2 µm) layer was deposited and patterned using standard metal etching techniques to form the bottom half of the electrical components of the sensor. A parylene diaphragm chamber was then created with photoresist as the sacrificial material. Gas-phase XeF_2 silicon roughening was conducted for strengthened adhesion between the parylene and the substrate. Another thick titanium/gold (200 Å/0.5 µm) layer was deposited and patterned on top of the parylene to realize the variable capacitor and variable capacitor/inductor structures by having different patterns of the sacrificial photoresist layer. For the variable capacitor, an additional parylene C layer was coated on the bottom metal before photoresist and parylene processes to reduce stray capacitance arising from the proximity of the two metal layers. Devices were finally released after performing a deep reactive-ion etch (DRIE) on the backside of wafer followed by photoresist stripping with acetone. Supercritical CO_2 drying was used to eliminate stiction of the free-standing parylene/metal/parylene diaphragm. Fig. 4 shows the microfabricated sensors with suture holes in 500 µm diameter at both ends for convenience in device anchoring during implantation.

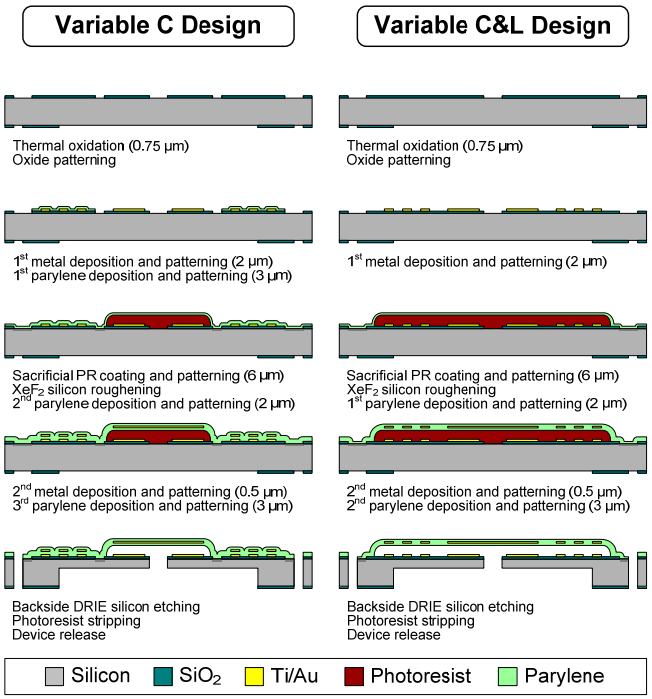

Figure 3. *Fabrication process flow.*

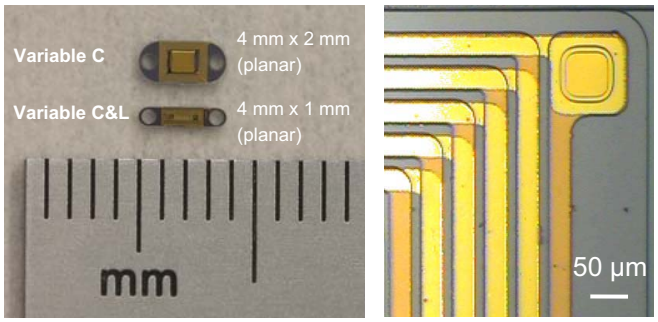

Figure 4. *Device images: (left) Microfabricated sensors; (right) Micrograph of the sandwiched metal/parylene/metal structure showing the via in the variable capacitor design.*

In order to enable successful device release and packaging, a special two-step etch mask with oxide and photoresist materials was used for the backside DRIE etching. By controlling the heights of this two-step mask, a backside recess was able to be formed on the substrate along with through-wafer etches on photoresist release holes beneath the parylene diaphragm chamber, the end anchor holes, and the release boundaries of the device. Therefore, a large cavity can be created inside the device after sealing the recess to encapsulate more air volume in addition to that in the surface-micromachined diaphragm chamber, which effectively increases pressure sensing capacity after packaging. For simplicity, the fabricated sensor device was glued to another non-electronic dummy piece with identical geometrical dimensions in this work, but undoubtedly the overall device thickness can be trimmed by thinning down the silicon pieces during fabrication. After packaging, a thin conformal parylene layer was finally coated on the device to enhance its biocompatibility.

4. RESULTS

Device testing was conducted using a 1.5-mm-diameter hand-wound coil connected to a HP4195A network analyzer to serve as the external reader for electrical measurements. Electrical parameters of the sensors were first obtained through lumped-model extraction by measuring the actual devices as well as several testing structures. Table I summarizes the experimental results which are in good agreement with theoretical calculations.

Table I *Electrical parameters of the microfabricated sensors*

	Variable C	Variable C&L
Resistance	~112 Ω	~72 Ω
Inductance	~0.78 μH	~0.36 μH
Capacitance	~8.5 pF	~3.1 pF
Resonant frequency	~62 MHz	~150 MHz
Quality factor at resonance	~3	~5

The wireless sensing distance is fundamentally limited by the quality factor of the device and the integrated coil size which affects inductive coupling efficiency with the reader coil. Even though the sensors have low quality factors (Q_s < 10) and small structural dimensions, their responses were still wirelessly detectable as shown in Fig. 5, thus validating the feasibility of the phase-dip technique as the sensing scheme. The maximum sensing distance in which the phase dip $\Delta\phi$ > 0.1°, defined by the noise floor from the testing system, was confirmed to be approximately 2 mm with sensors in both designs. Other than reader optimization, the following strategies directly related to device can improve the sensing distance and should be included in future development: (1) increase of integrated coil size ($k\uparrow$); (2) increase of metal line thickness ($R_s\downarrow$); (3) increase of insulating oxide thickness or modification of substrate material ($C_s\downarrow$).

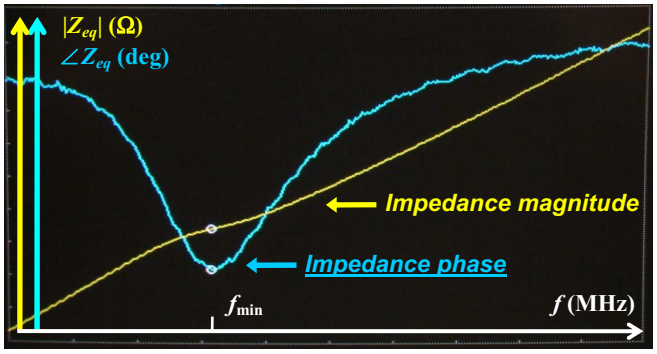

Figure 5. *Captured frequency scan example of equivalent impedance Z_{eq} of the reader coil coupled with the sensor.*

After electrical characterization the sensors were tested on-chip to measure their pressure responses. Pressure differences were generated by introducing pressurized air to the inside of the sensor diaphragm chamber through a customized packaging jig connected to a controllable pressure regulation system with constant environmental pressure outside the diaphragm chamber. Experimental results as shown in Fig. 6 successfully demonstrate highly sensitive pressure responses on because of high compliance of the parylene flexible diaphragm and high resonant frequency of the sensors. For sensors of the variable capacitor design, the measured data points were fit using the following relation with the assumption of small diaphragm deflection proportional to pressure difference:

$$\frac{f_{\min}(\Delta P)}{f_{\min}(\Delta P=0)} = \frac{\dfrac{1}{2\pi\sqrt{L_s(C_s-\Delta C_s)}}}{\dfrac{1}{2\pi\sqrt{L_s C_s}}} \cong (1+\alpha\Delta P)^{1/2}$$

where α is the fitting parameter. The same procedures on normalized resonant frequency analysis were applied to sensors of the variable capacitor/inductor design under small deflection assumption with the relation between mutual inductance and separation distance in conductors [9]:

$$\frac{f_{\min}(\Delta P)}{f_{\min}(\Delta P=0)} = \frac{1}{\sqrt{1-\Delta L_s/L_s}}\frac{1}{\sqrt{1-\Delta C_s/C_s}} \cong (1+\beta_1\Delta P+\beta_2\Delta P)^{1/2}$$

where β_1 and β_2 are also the fitting parameters describing more sensitive pressure response due to the coupled capacitance and inductance variations. Data analysis confirms that sensors of the both designs achieved excellent pressure sensing performance with high sensitivities (> 7000 ppm/mmHg) and mmHg level resolution in a measurement range of more than 0-30 mmHg, which sufficiently covers all IOP variations of interest in practical monitoring.

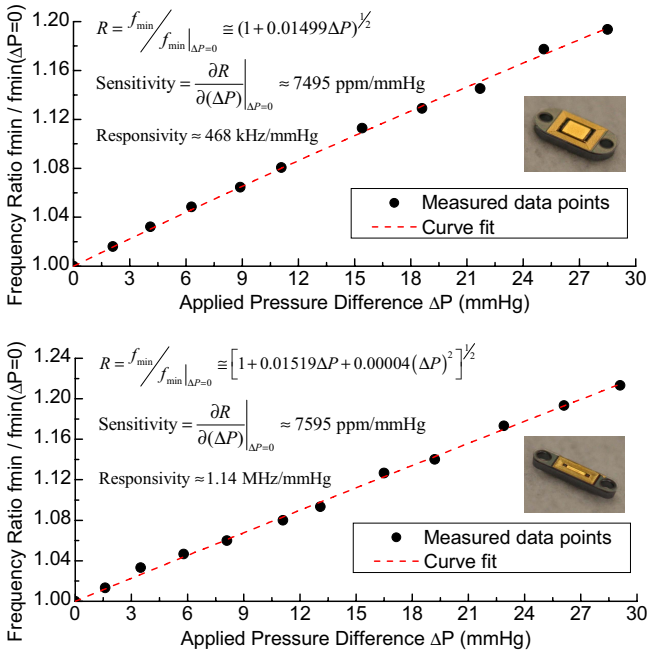

Figure 6. *Pressure testing results of the on-chip sensors with variable capacitor (top) and variable capacitor/inductor (bottom) designs.*

In vivo testing was conducted using a live rabbit eye as the model to evaluate the bioefficacy and biostability of the sensor implant. The device was implanted at a pars plana site to reduce the required sensing distance to the external coil. Its end anchor holes facilitate robust device anchoring with use of sutures during device implantation. Results as shown in Fig. 7 indicate no surgical complications, inflammatory responses, or device encapsulation after more than 150 days, which verifies device biocompatibility in the intraocular environment. Extensive animal studies including *in vivo* pressure sensing demonstration and optimal device placement investigation will be performed in future work.

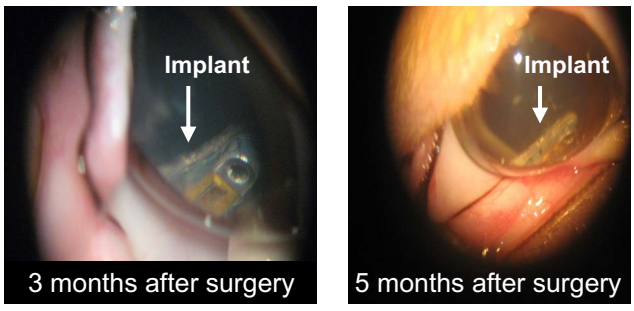

Figure 7. *In vivo device testing using a live rabbit eye model.*

5. CONCLUSION

A novel implantable wireless intraocular pressure sensor has been successfully developed featuring parylene as the biocompatible/implantable structural material. Sensors with resonant circuitry involving pressure-sensitive variable capacitor and variable capacitor/inductor designs were implemented to facilitate wireless pressure sensing by creating an inductive coupling link with the external reader. A low-temperature multi-layer micromachining technology enables integrated sensor components fabricated on a monolithic substrate without the need of wafer bonding process. Sensors with implantable planar dimensions (4 mm x 2 mm in variable capacitor and 4 mm x 1 mm in variable capacitor/inductor design) were microfabricated in a suitable form factor for intraocular implantation. On-bench device testing achieved successful pressure sensing with more than 7000 ppm/mmHg sensitivity and 1 mmHg resolution. Biocompatibility of the device implant was successfully verified through *in vivo* characterization in live animal study, which provides evidence that the sensors can be utilized for long-term continuous IOP monitoring in glaucoma patients.

ACKNOWLEDGEMENTS

This work was supported in part by the Engineering Research Centers Program of the National Science Foundation (Award Number EEC-0310723) and part by Bausch and Lomb. The authors especially thank Dr. Rajat Agrawal and Dr. Rohit Varma for their valuable comments on surgical procedures, and Mr. Trevor Roper for his fabrication assistance.

REFERENCES

[1] M. Yanoff and J.S. Duker (Eds.), *Ophthalmology*, Second Edition, Mosby, St. Louis, 2003.

[2] C.C. Collins, "Miniature Passive Pressure Transensor for Implanting in the Eye," *IEEE Transactions on Biomedical Engineering*, BME-14(2), pp. 74-83, 1967.

[3] L. Rosengren, P. Rangsten, Y. Bäcklund, B. Hök, B. Svedbergh, and G. Selén, "A System for Passive Implantable Pressure Sensors," *Sensors and Actuators A: Physical*, 43(1-3), pp. 55-58, 1994.

[4] O. Akar, T. Akin, and K. Najafi, "A Wireless Batch Sealed Absolute Capacitive Pressure Sensor," *Sensor and Actuators A: Physical*, 95(1), pp. 29-38, 2001.

[5] A. DeHennis and K.D. Wise, "A Double-Sided Single- Chip Wireless Pressure Sensor," *Proc. MEMS 2002*, pp. 252-255.

[6] A. Baldi, W. Choi, and B. Ziaie, "A Self-Resonant Frequency-Modulated Micromachined Passive Pressure Transensor," *IEEE Sensors Journal*, 3(6), pp. 728-733, 2003.

[7] M.A. Fonseca, M.G. Allen, J. Kroh, and J. White, "Flexible Wireless Passive Pressure Sensors for Biomedical Applications," *Proc. Hilton Head 2006*, pp. 37-42.

[8] J. Shih, J. Xie, and Y.-C. Tai, "Surface Micromachined and Integrated Capacitive Sensors for Microfluidic Applications," *Proc. Transducers 2003*, pp. 388-391.

[9] F.E. Terman, *Radio Engineers' Handbook*, McGraw-Hill, New York, 1943.

[10] T.H. Lee, *The Design of CMOS Radio-Frequency Integrated Circuits*, Second Edition, Cambridge University Press, New York, 2004.